Dual Roles for RHOA/RHO-Kinase In the Regulated Trafficking of a Voltage-sensitive Potassium Channel

Lee Stirling, Michael R. Williams, and Anthony D. Morielli

Department of Pharmacology, College of Medicine, University of Vermont, Burlington, VT 05405

Kv1.2 is a member of the *Shaker* family of voltage-sensitive potassium channels and contributes to regulation of membrane excitability. The electrophysiological activity of Kv1.2 undergoes tyrosine kinase-dependent suppression in a process involving RhoA. We report that RhoA elicits suppression of Kv1.2 ionic current by modulating channel endocytosis. This occurs through two distinct pathways, one clathrin-dependent and the other cholesterol-dependent. Activation of Rho kinase (ROCK) via the lysophosphatidic acid (LPA) receptor elicits clathrin-dependent Kv1.2 endocytosis and consequent attenuation of its ionic current. LPA-induced channel endocytosis is blocked by the ROCK inhibitor Y27632 or by clathrin RNA interference. In contrast, steady-state endocytosis of Kv1.2 in unstimulated cells is cholesterol dependent. Inhibition of basal ROCK signaling with Y27632 increased surface Kv1.2, an effect that persists in the presence of clathrin small interfering RNA and that is not additive to the increase in surface channel levels elicited by the cholesterol sequestering drug filipin. Temperature block experiments show that ROCK affects cholesterol-dependent trafficking by modulating the recycling of endocytosed channel back to the plasma membrane. Both receptor-stimulated and steady-state Kv1.2 trafficking modulated by RhoA/ROCK required the activation of dynamin as well as the ROCK effector Lim-kinase, indicating a key role for actin remodeling in RhoA-dependent Kv1.2 regulation.

INTRODUCTION

The voltage-gated potassium channel Kv1.2 regulates diverse physiological functions, including the maintenance of action potential proliferation along myelinated axons (Rasband *et al.*, 2001, 2004; Rasband and Trimmer, 2001; Rasband, 2004), transduction of pain in peripheral sensory neurons (Feng *et al.*, 1999; Kim *et al.*, 2002; Yang *et al.*, 2004), and modulation of tone in vascular smooth muscle (Adda *et al.*, 1996; Wang *et al.*, 1997, 2005). Dysregulation of Kv1.2 has been implicated in disease states such as hypertension (Cox *et al.*, 2001; Hong *et al.*, 2004), neuropathic pain (Ishikawa *et al.*, 1999; Kim *et al.*, 2002; Yang *et al.*, 2004), and seizure activity in the CNS (Lambe and Aghajanian, 2001; Brew *et al.*, 2007). Kv1.2 is important for maintaining neuronal resting membrane potential (Dodson *et al.*, 2003) and is heavily expressed in neurons of the hippocampus and cerebellum (Tsaur *et al.*, 1992; Sheng *et al.*, 1994; Veh *et al.*, 1995; Grosse *et al.*, 2000) in which it influences neuron firing (Laube *et al.*, 1996; Southan and Robertson, 1998; Haghdoust *et al.*, 2007). Commensurate with its role as a regulator of cellular physiology, Kv1.2 is itself highly regulated. Understanding the pathways involved in Kv1.2 regulation is therefore fundamental to understanding of an array of physiological processes.

Kv1.2 is subject to both positive and negative regulation. Negative regulation of Kv1.2 involves tyrosine phosphorylation-dependent suppression of its ionic current (Huang *et al.*, 1993). This can occur in response to a variety of stimuli,

including the activation of G-protein coupled receptors (Huang *et al.*, 1993). Channel suppression by this pathway requires the activity of the small GTPase RhoA (Cachero *et al.*, 1998); inhibition of RhoA GTPase activity with C3 exoenzyme or overexpression of a dominant negative form of RhoA prevents the suppression of Kv1.2 ionic current in response to channel tyrosine phosphorylation (Cachero *et al.*, 1998). The finding that RhoA modulates Kv1.2 was significant because it provided a new link between signaling pathways governing actin dynamics and pathways governing membrane excitability. For example, in vascular smooth muscle, both RhoA and Kv1.2 regulate contractility. In this tissue, it is well accepted that RhoA acts through direct effects on the contractile machinery (Uehata *et al.*, 1997; Nakamura *et al.*, 2003) and that Kv1.2 affects contractility indirectly through its effects on membrane potential (Yuan, 1995; Yuan *et al.*, 1998). The finding that RhoA affects Kv1.2 function raised the intriguing possibility that the effects of Kv1.2 and RhoA on smooth muscle contractility may not be distinct but instead may be tightly connected. Subsequent studies have begun to support this idea (Luykenaar *et al.*, 2004). Similar links may exist between RhoA-regulated actin dynamics and membrane potential in other tissues expressing Kv1.2, including neuronal synapses (Dodson *et al.*, 2003). Despite the evident importance of this signaling nexus, the mechanism by which RhoA regulates Kv1.2 is not known.

Tyrosine phosphorylation-dependent suppression of Kv1.2 ionic current involves endocytosis of the channel protein from the cell surface (Nesti *et al.*, 2004). Kv1.2 endocytosis has at least two distinct components: steady-state channel endocytosis and receptor-induced endocytosis (Williams *et al.*, 2007; Connors *et al.*, 2008). Both forms of Kv1.2 endocytosis require direct association of Kv1.2 with the actin-regulating protein cortactin (Hattan *et al.*, 2002; Williams *et al.*, 2007). Strikingly, each pathway is affected by distinct actin-regulatory domains within cortactin (Williams *et al.*,

2007). Disruption of the F-actin binding region within cortactin affects steady-state and receptor induced channel endocytosis. In contrast, disruption of the ability of cortactin to stimulate dendritic actin polymerization via Arp2/3 selectively blocks receptor-induced channel endocytosis but has no effect on steady-state channel trafficking. Despite being clearly separable based on distinct actin-regulatory functions of cortactin, the mechanisms involved in steady-state versus receptor-induced Kv1.2 endocytosis have remained unclear.

Because Kv1.2 regulation involves actin-dependent endocytosis, and because RhoA is a key modulator of both actin dynamics and endocytosis, we hypothesized that RhoA affects Kv1.2 ionic current by modulating channel endocytosis. This idea is consistent with involvement of RhoA in the trafficking of a variety of other membrane proteins. For example, in alveolar epithelial cells clathrin-dependent Na,K-ATPase endocytosis in response to hypoxia is dependent upon RhoA activation (Dada *et al.*, 2007), in HeLa cells activation of RhoA inhibits clathrin-dependent endocytosis of epidermal growth factor (EGF) and transferrin (Tf) receptors (Lamaze *et al.*, 1996), and in lymphocytes RhoA is required for clathrin-independent, cholesterol-dependent internalization of interleukin-2 receptors (Symons and Rusk, 2003). In some instances, RhoA modulation of endocytosis involves Rho-kinase (ROCK). Perhaps the most well understood RhoA effector, ROCK is a serine/threonine kinase that is activated by RhoA (Ishizaki *et al.*, 1996; Matsui *et al.*, 1996). Examples of RhoA/ROCK-dependent endocytosis include a requirement for ROCK in Na,K-ATPase endocytosis in alveolar epithelial cells (Dada *et al.*, 2007) and for rearward clathrin structure polarization during the migration of T lymphocytes (Samaniego *et al.*, 2007). ROCK activation inhibits epidermal growth factor (EGF) receptor endocytosis in a process involving LIM-kinase/cofilin (Kaneko *et al.*, 2005). In this pathway, RhoA activates ROCK, which in turn phosphorylates and activates LIM-kinase. LIM-kinase then phosphorylates its only known substrate, the F-actin–severing protein cofilin, thereby inactivating it (Bernard, 2007), leading to alteration of actin dynamics and modulation of endocytosis. This finding is crucial because it provides a direct link between regulated actin dynamics and RhoA-mediated endocytosis. Despite these intriguing findings, evidence linking RhoA, actin dynamics, and endocytosis remains sparse.

Here, we report that RhoA is a determinant of Kv1.2 trafficking. We show that RhoA activity is inversely correlated to the level of channel at the cell surface and that this reduction in surface Kv1.2 levels occurs through channel endocytosis. Our findings reveal that steady-state homeostasis of Kv1.2 is achieved through a balance of constitutive, cholesterol-dependent endocytosis and channel recycling that is distinct from clathrin-dependent channel endocytosis elicited by G protein-coupled lysophosphatidic acid (LPA) receptor activation. RhoA/ROCK signaling contributes to both forms of Kv1.2 trafficking but does so through distinct mechanisms in each case. In addition, we demonstrate that dynamin is necessary for both forms of Kv1.2 trafficking. Finally, we show that RhoA/ROCK modulates Kv1.2 trafficking through LIM-kinase/cofilin, thus establishing a direct link between RhoA-regulated actin dynamics and the functional regulation of Kv1.2.

MATERIALS AND METHODS

Materials

Rabbit polyclonal antibody directed against the first extracellular loop of Kv1.2 (α-Kv1.2e) was developed in conjunction with BioSource International (Camarillo, CA). Eary endosomal antigen (EEA) 1 monoclonal (α-EEA1m) and clathrin heavy chain monoclonal (α-CHCm) antibodies were purchased from BD Biosciences (Franklin Lakes, NJ). RhoA rat monoclonal antibody (mAb) (α-RhoA) was a generous gift of Dr. S. Yonemura (Center for Developmental Biology, RIKEN, Kobe, Japan). Phospho-MYPT1 (α-pMYPT1p) polyclonal and glyceraldehyde-3-phosphate dehydrogenase (GAPDH) (α-GAPDHm) monoclonal antibodies were purchased from Millipore (Billerica, MA). Alexa Fluor-conjugated transferrin, secondary antibodies, and phalloidin were purchased from Invitrogen (Carlsbad, CA). Nontargeting small interfering RNA (siRNA) and clathrin heavy chain siRNA were purchased from Dharmacon RNA Technologies (Lafayette, CO). Y27632 was purchased from EMD Biosciences (San Diego, CA), cell-permeable C3 exoenzyme (CT04) was purchased from Cytoskeleton (Denver, CO), and LPA and filipin were purchased from Sigma-Aldrich (St. Louis, MO). RhoA (T19N), ROCK (RB/PH-TT), LIM-kinase (D460A), and Cofilin (S3A) were generously provided by Dr. K. Hahn (University of North Carolina at Chapel Hill, Chapel Hill, NC), Dr. K. Kaibuchi (Nagoya University, Nagoya, Japan), Dr. K. Suzuki (National Institute of Health Sciences, Tokyo, Japan), and Dr. P. Caroni (Friedrich Miescher Institute, Basel, Switzerland) respectively. Dynasore was generously provided by Dr. T. Kirchhausen (Harvard Medical School, Boston, MA).

Cell Culture and Transfections

Human embryonic kidney 293 cells stably expressing Kv1.2-α, Kvβ2, and the M1 muscarinic acetylcholine receptor (HEK-K) were used and cultured as reported previously (Nesti *et al.*, 2004). Experimental plasmid constructs were cotransfected into HEK-K cells with pEGFP-N1 by using calcium phosphate. Confluent cultures were plated to a density of 3.3×10^4 cells/cm^2 onto tissue culture plates or glass coverslips (Corning, Corning, NY) coated with poly-D-lysine (Sigma-Aldrich) (0.1 mg/ml) or plasma fibronectin (0.015 mg/ml) for biochemistry, flow cytometry, electrophysiology, and immunofluorescence 12–16 h in serum-free media before use.

Electrophysiology

All recordings were made on HEK-K cells using the whole-cell patch-clamp method. Data were collected using an Axopatch 200 patch-clamp amplifier using pClamp 9.2 (Axon Instruments, Burlingame, CA). Currents were collected with step pulses from −70 to +50 mV in increments of 10 mV from a holding potential of −60 mV and were leak subtracted with a P/4 protocol. The pipette solution contained 60 mM K$_2$SO$_4$, 1.2 mM KCl, 5 mM MgSO$_4$, 5 mM Na-HEPES, and 35 mM sucrose, pH 7.1. The external (bath) solution contained 118 mM NaCl, 2.5 mM KCl, 1.8 mM CaCl$_2$, 0.8 mM MgCl$_2$, 5 mM Na-HEPES, and 23 mM glucose, pH 7.4. All recordings were made at 37°C.

Detection of Surface Kv1.2

For flow cytometric detection of surface Kv1.2, HEK-K cells were treated with a saline, a vehicle control solution, or an appropriate stimulus, and then 154 mM sodium azide as described in Nesti *et al.* (2004). After azide, the cells were lifted and placed in a test tube where surface Kv1.2 was labeled with 0.33 μg/ml α-Kv1.2e. Antibody binding was detected with fluorescently conjugated anti-rabbit immunoglobulin G (IgG) (0.1 μg/ml). Fluorescence was detected by flow cytometry as described below.

Flow Cytometry

A single laser flow cytometer (Easy Cyte PCA-96; Guava Technologies, Hayward, CA) was used. In all HEK-K cells, α-Kv1.2e primary antibody was detected by labeling with a goat α-rabbit secondary antibody conjugated to phycoerythrin/Cy5, with an excitation peak of 488 nm and an emission peak of 667 nm (Southern Biotechnology Associates, Birmingham, AL). Surface Kv1.2 in transfected cells was taken as the distribution of cells emitting at 667 nm (indicating surface Kv1.2) in cells also emitting at 508 nm (indicating green fluorescent protein [GFP] expression) minus background signal. Background staining was quantified by replacing α-Kv1.2e with the same concentration of rabbit serum IgG. Internalization of Kv1.2 was detected as described previously (Nesti *et al.*, 2004). Cells were exposed to α-Kv1.2e prelabeled with Zenon-488 (Invitrogen) for 10 min followed by washout. Cells were then incubated at 37°C for an additional 10 min, followed by acid wash to remove antibody remaining on the cell surface. Remaining fluorescence from internalized channel was detected by flow cytometry.

Immunoblot

Western analysis of HEK-K whole cell lysates was performed as reported previously (Connors *et al.*, 2008).

Immunofluorescence

Confluent cultures were plated as for flow cytometry and pretreated as indicated at 37°C. α-Kv1.2e was applied to live cells at 0.33 μg/ml for 10 min at 37°C. Cells were fixed with 4% paraformaldehyde (Polysciences, Warrington, PA) in PHEM 6.1 buffer (60 mM PIPES, 25 mM HEPES, 2 mM MgCl$_2$, and 10 mM EGTA, pH to 6.1 with KOH) at room temperature. Cells were extracted with ice-cold acetone. Coverslips were incubated in blocking buffer (PHEM 6.9, 3% goat serum, and 0.1% fish skin gelatin) at room temperature.

Figure 1. RhoA activity can modulate levels of Kv1.2 at the cell surface. (A) Application of increasing concentrations of C3 exoenzyme (6 h) significantly increases the level of cell surface Kv1.2 as detected by flow cytometry in HEK-K cells (n = 4; *p < 0.05, **p < 0.01). (B) Transient transfection with increasing amounts of DNA encoding a dominant negative form of RhoA (T19N) significantly increases the level of steady-state surface Kv1.2 in a concentration-dependent manner (n = 18; **p < 0.001). (C) Steady-state internalization of Kv1.2 detected by flow cytometry is blocked

in cells pretreated with C3 exoenzyme relative to untreated control cells (n = 9; *p < 0.001). The inset shows an immunoblot of the same cells used for flow cytometry, probed with Kv1.2 or GAPDH.
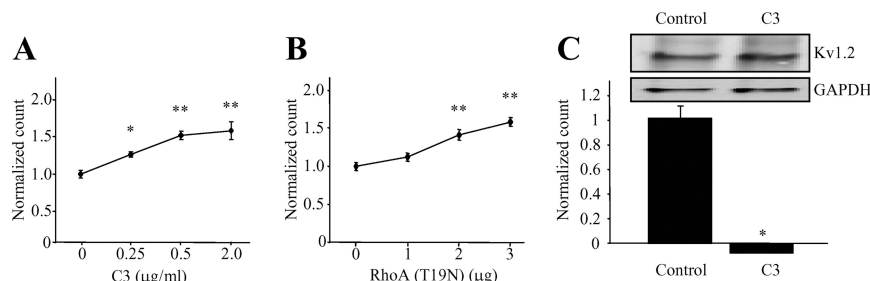
Other primary antibodies were then applied (α-EEA1, 1.25 μg/ml; α-RhoA, 35.1 μg/ml; α-CHCm, 2.5 μg/ml) diluted in blocking buffer. Alexa Fluor-conjugated secondary antibodies were applied (4 μg/ml in blocking buffer) (Invitrogen) at room temperature. F-Actin was detected with Alexa Fluor 350 phalloidin (Invitrogen) (4 U/ml). Coverslips were mounted on glass slides with ProLong Gold mounting medium (Invitrogen) according to the provided protocol. Images were obtained with the DeltaVision reconstruction microscopy system (Applied Precision, Issaquah, WA).

Transferrin Endocytosis Assay

Confluent cultures were plated as for flow cytometry. Coverslips were washed with warm serum-free media, chilled, and then incubated for 45 min in cold serum-free media containing 25 μg/ml Alexa 488-conjugated transferrin. Coverslips were washed then moved to 37°C for 0 or 15 min. Coverslips were chilled, washed, and processed for immunofluorescence.

Statistical Analysis

Descriptive statistics are provided in figures as line or bar graphs indicating the sample mean with error bars indicating the SEM. Detection of statistical difference between two independent measurements was by one-way t test. Comparison of percent changes between pairs of independent measurements was by two-way analysis of variance (ANOVA). Sample populations were considered to be significant at p ≤ 0.05.

RESULTS

RhoA Affects the Surface Expression of Kv1.2

Tyrosine kinase-dependent suppression of Kv1.2 by M1 muscarinic acetylcholine receptors requires RhoA (Cachero *et al.*, 1998). In independent studies, this process has been shown to occur by channel endocytosis from the plasma membrane (Nesti *et al.*, 2004; Williams *et al.*, 2007; Connors *et al.*, 2008). However, it is not known whether these two processes are mechanistically linked. We therefore asked whether Kv1.2 trafficking at the plasma membrane requires RhoA. Using flow cytometry as described previously (Nesti *et al.*, 2004; Williams *et al.*, 2007; Connors *et al.*, 2008), steady-state levels of Kv1.2 at the cell surface were measured in the presence and absence of the RhoA-specific inhibitor C3 exoenzyme. Treatment of HEK-K cells with increasing concentrations of C3 exoenzyme produced a concentration-dependent increase of steady-state surface Kv1.2 levels at the cell surface (Figure 1A) (n = 4; *p < 0.05, **p < 0.01). In a complementary experiment designed to confirm that the C3 exoenzyme effect is specific to RhoA, increasing amounts of dominant-negative RhoA (T19N) (Subauste *et al.*, 2000) were transfected. This too caused a dose-dependent increase of steady-state surface Kv1.2 levels (Figure 1B) (n = 18, **p < 0.001). In a previous study, we demonstrated that in quiescent, serum-starved HEK cells, Kv1.2 channels at the cell surface undergo steady-state endocytosis even in the absence of stimuli that elicit acute internalization (Nesti *et al.*, 2004). We therefore tested the hypothesis that C3 exoenzyme or RhoA (T19N) increase surface Kv1.2 levels by inhibiting steady-

state channel endocytosis. Steady-state Kv1.2 endocytosis was measured using flow cytometry as described under *Materials and Methods*. Surface Kv1.2 channels were bound to a fluorescence-labeled α-Kv1.2e antibody and allowed to undergo steady-state endocytosis for 10 min, after which time the surface antibody was removed by acid wash. The remaining fluorescence derives from labeled Kv1.2 channels that had been internalized. Figure 1C shows flow cytometric detection of internalized fluorescence in control cells but not in cells pretreated with C3 exoenzyme (n = 9; *p < 0.001). These data indicate that the level of Kv1.2 at the surface of quiescent cells is modulated by RhoA-dependent of steady-state channel endocytosis.

RhoA Activation Triggers Kv1.2 Endocytosis

The LPA receptor couples to $G_{12/13}$ to potently activate RhoA (Moolenaar, 1995; Bian *et al.*, 2006). Stimulation of endogenous LPA receptors in HEK-K cells elicited a significant, concentration-dependent reduction of surface Kv1.2 (Figure 2A) (n = 5; *p < 0.05, **p < 0.01). Whole-cell patch-clamp studies confirmed that the loss of surface Kv1.2 induced by LPA (10 μM; 15 min) correlated with a reduction of Kv1.2 function. The mean steady-state current amplitude measured between 60 and 80 ms after depolarization to +20 mV was reduced from 9.4 ± 1.1 mV in saline-treated cells to 4.3 ± 1.4 mV in cells treated with LPA (Figure 2B) (n ≥ 11, p < 0.01). To determine whether the LPA effect on Kv1.2 surface expression results from its ability to activate RhoA, cells were pretreated with C3 exoenzyme to block RhoA before treatment with LPA. In control cells not pretreated C3 exoenzyme, LPA reduced surface channel levels by ~50% (Figure 2C) (n = 9; *p < 0.001). In cells pretreated with 2 μg/ml C3 exoenzyme for 6 h, LPA had no significant effect on surface channel levels (n = 9; p = 0.37). Therefore, LPA-induced reduction of Kv1.2 channels at the cell surface requires active RhoA.

M1 muscarinic acetylcholine receptor stimulation caused endocytosis of Kv1.2 to EEA1-containing structures (Nesti *et al.*, 2004). To confirm that LPA-induced loss of surface Kv1.2 also occurs by channel endocytosis, immunofluorescence was used to visualize Kv1.2 trafficking in HEK-K cells treated with saline or LPA. Surface Kv1.2 was labeled in live cells with α-Kv1.2e before addition of saline or LPA (10 μM; 15 min), followed by fixation and analysis by immunofluorescence. Fixed cells were probed Alexa-350 phalloidin and with rat polyclonal α-RhoA and mouse α-EEA1 antibodies. α-Kv1.2e was detected with an anti-rabbit secondary and α-RhoA and α-EEA1 were detected with anti-rat or anti-mouse secondary antibodies, respectively. LPA treatment resulted in translocation of Kv1.2 from the cell periphery to

A

B

C

D

5 microns
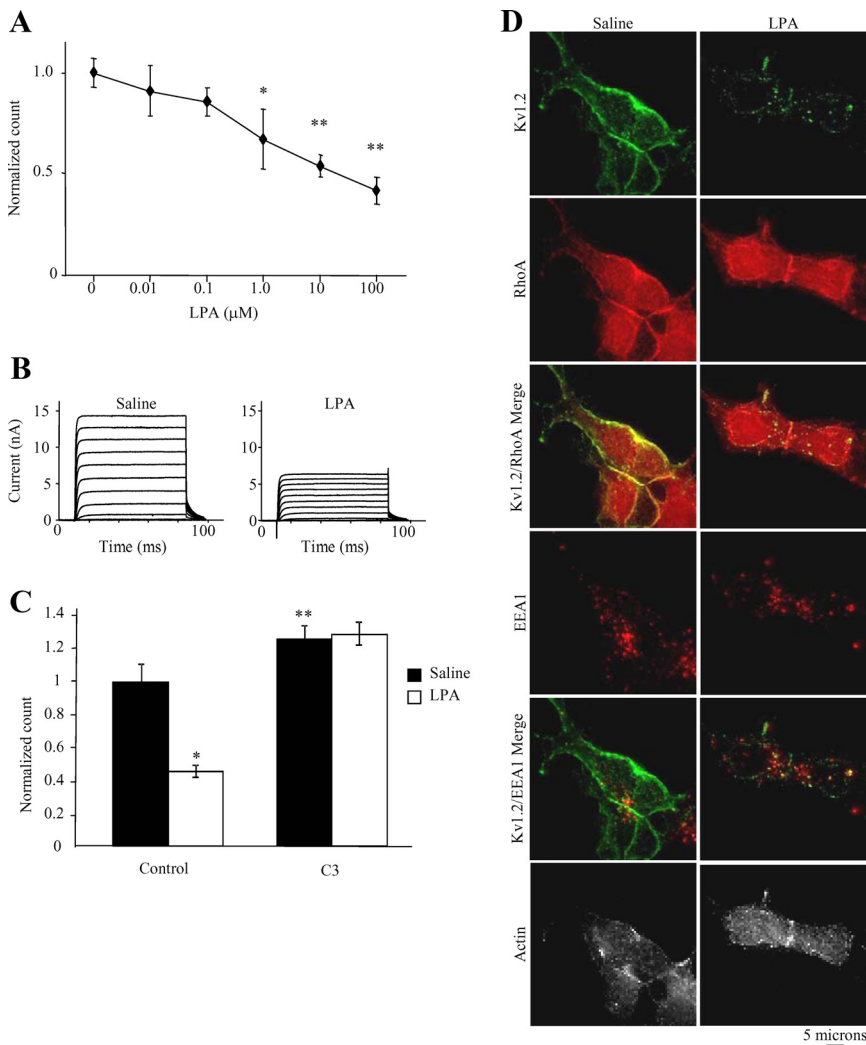
Figure 2. Activation of RhoA triggers Kv1.2 endocytosis. (A) Application of increasing concentrations of LPA (15 min) significantly reduces the level of Kv1.2 at the cell surface in a concentration-dependent manner as detected by flow cytometry (n = 5' *p < 0.05, **p < 0.01). (B) Average whole-cell currents evoked in HEK-K cells with pulses from −70 to +50 mV in increments of 10 mV in the presence of saline or LPA (10 μM; 15 min). LPA application significantly reduces mean whole-cell currents. Current traces for each condition represent the average of at least 11 cells (n ≥11; p < 0.01). (C) Pretreatment of HEK-K cells with C3 exoenzyme (2 μg/ml; 6 h) significantly increases steady-state surface Kv1.2 (n = 9; **p = 0.028). LPA caused a significant decrease in surface Kv1.2 levels in control cells (C) (n = 9; *p < 0.001) but had no significant effect in cell pre-treated with C3 exoenzyme (n = 9, p = 0.37). (D) In HEK-K cells, LPA application results in translocation of Kv1.2 (green) from the RhoA and actin rich edge of the cell (left column) to intracellular puncta that contain EEA1 or are adjacent to EEA1-containing structures (right column).

intracellular puncta. Internalized Kv1.2 puncta costained with EEA1 or were adjacent to EEA1-containing structures (Figure 2E), confirming that LPA treatment elicited channel endocytosis. These data support the hypothesis that RhoA exerts its effect on channel function by modulating channel endocytosis.

ROCK Is Required for LPA-induced Kv1.2 Endocytosis

A major downstream effector of RhoA is ROCK, a serine/threonine kinase that modulates the actin cytoskeleton and regulates the trafficking of membrane proteins (Narumiya *et al.*, 1997; Kaneko *et al.*, 2005; Dada *et al.*, 2007; Samaniego *et al.*, 2007). To test the hypothesis that RhoA effects on Kv1.2 involve ROCK, we took two distinct approaches to inhibiting ROCK. First, DNA encoding a dominant-negative form of ROCK (RB/PH-TT) (Amano *et al.*, 1999) was transfected into HEK-K cells and the effect on Kv1.2 surface levels and trafficking was determined. Overexpression of dominant-negative ROCK resulted in a significant increase in levels of Kv1.2 at the cell surface in unstimulated cells (Figure 3A) (n = 69; **p < 0.001). LPA produced a significant reduction in surface channel in both control cells and cells expressing dominant-negative ROCK (n = 69; p < 0.01); however, two-way ANOVA reveals that the percent change in surface Kv1.2 evoked by LPA in control cells was significantly less

than that evoked by LPA in cells expressing dominant-negative ROCK (Figure 3A, inset) (n = 69; **p < 0.001). Therefore, overexpression of dominant-negative ROCK caused a partial, but strongly significant inhibition of LPA-induced channel endocytosis. Such partial inhibition could arise from an inability to achieve high enough expression of ROCK (RB/PH-TT) to fully interfere with endogenous ROCK function or from the presence of a ROCK-independent pathway. We therefore took the complementary approach of blocking ROCK with the pharmacological inhibitor Y27632. Inhibiting ROCK in this way also significantly increased the steady-state level of surface Kv1.2 (Figure 3B) (n = 40; *p < 0.01, **p < 0.001) but completely blocked LPA-induced Kv1.2 endocytosis (Figure 3B) (n = 40; *p < 0.01, **p < 0.001). To confirm that LPA activates ROCK and that Y27632 exerts its effect on Kv1.2 by inhibiting that activation, we used Thr696-phosphorylated myosin phosphatase-1 (MYPT1) as an indirect measure of ROCK activity (Feng *et al.*, 1999). LPA treatment (10 μM; 15 min) of HEK-K cells increased detectable pMYPT1, whereas treatment with the ROCK inhibitor Y27632 (10 μM; 30 min) reduced levels of pMYPT1 relative to saline control (Figure 3B, right inset). Immunofluorescence experiments shown in Figure 3D confirm that the effects on surface Kv1.2 observed in flow cytometry experiments (Figure 3B) arise from alterations in
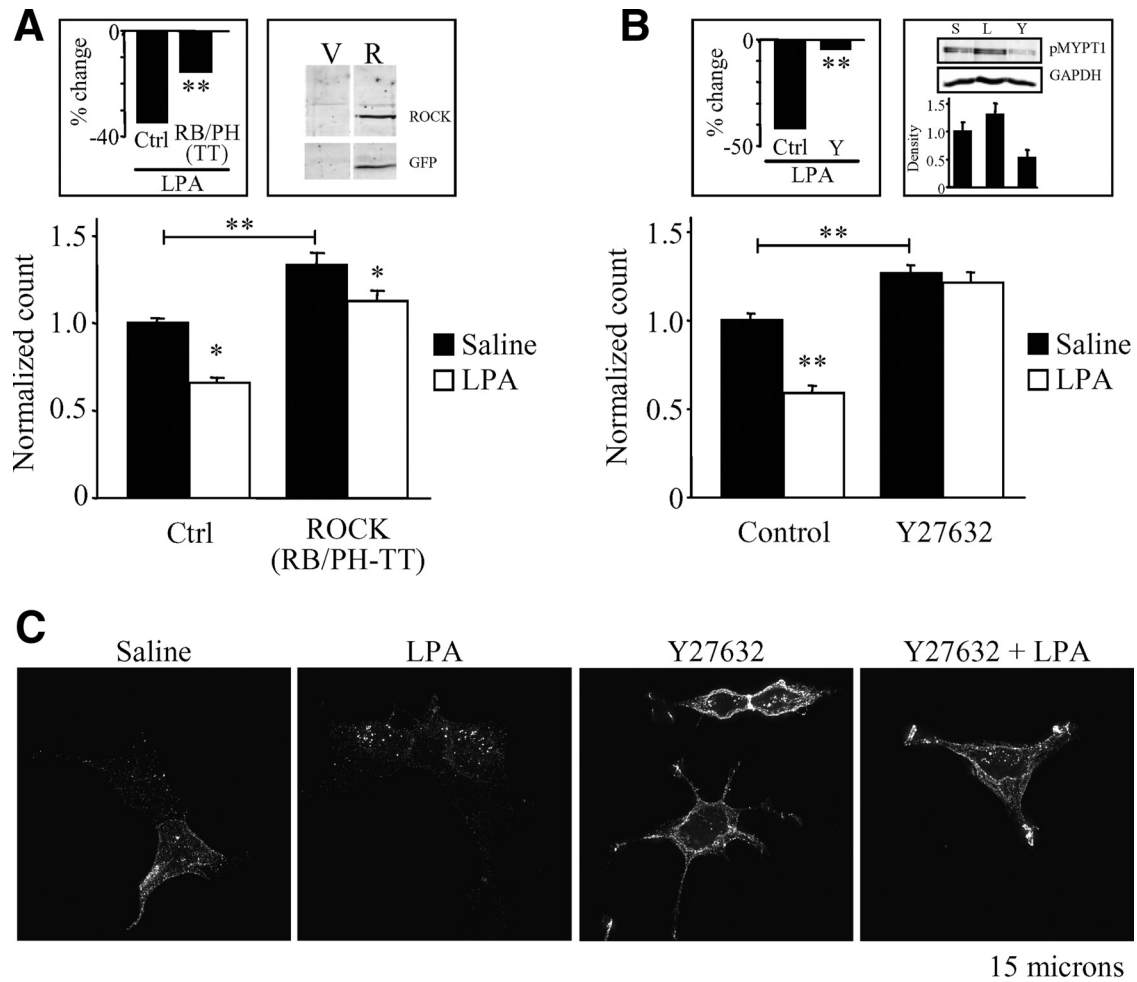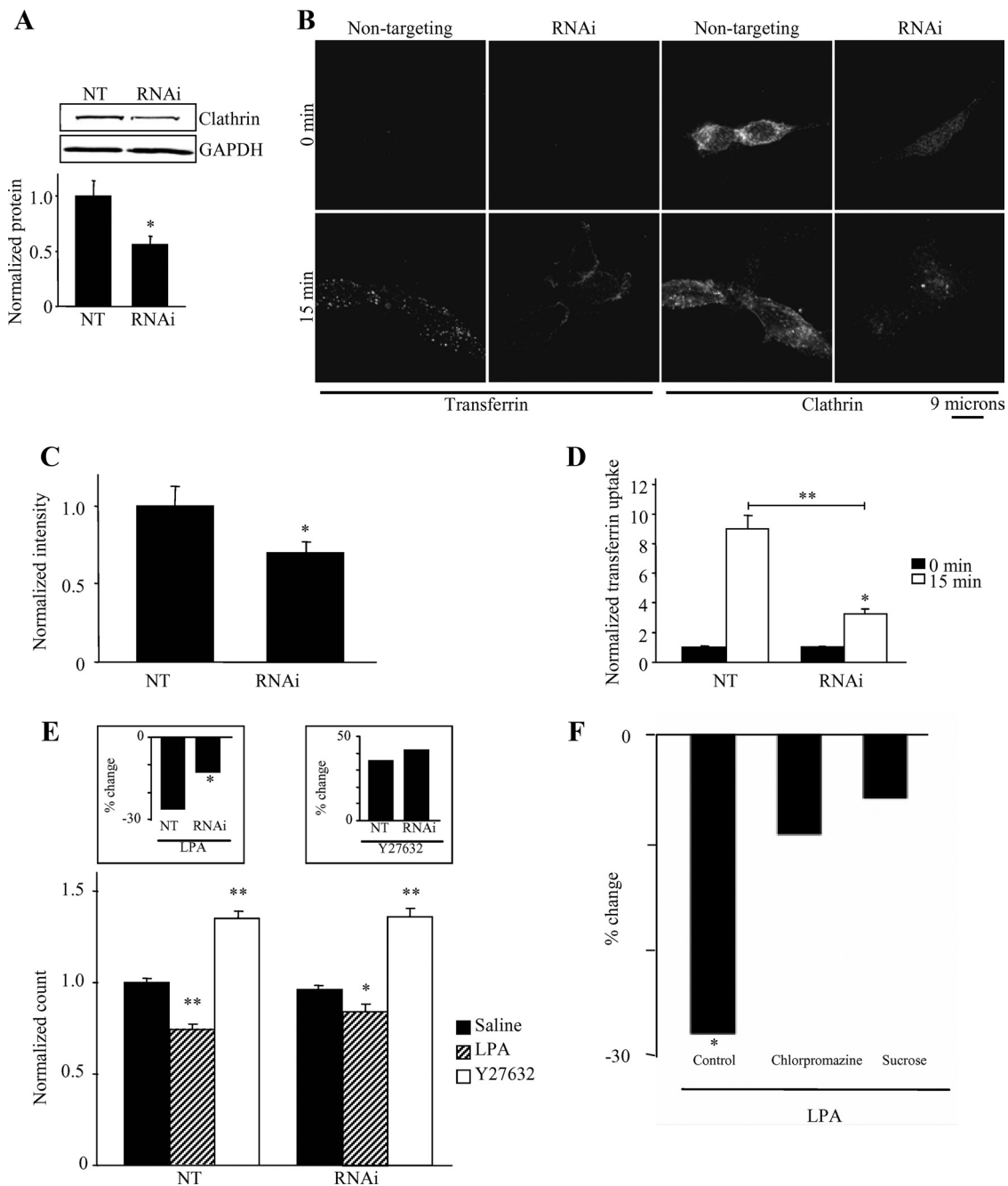
Figure 3. LPA-induced endocytosis of Kv1.2 requires ROCK activation. (A) Overexpression of a dominant negative form of ROCK (RB/PH-TT) in HEK-K cells significantly increases steady-state levels of surface Kv1.2 and reduced the change elicited by LPA (n = 69; *p < 0.05, **p < 0.001). Left, inset, percentage change in surface Kv1.2 elicited by LPA is significantly reduced cells expressing RB/PH-TT relative to control (n = 69; **p < 0.001). Right, inset, expression of RB/PH-TT is confirmed by immunoblot probed with anti-GFP in vector (V) or RB/PH-TT (R) transfected cells. (B) Pretreatment with the ROCK inhibitor Y27632 (10 μM; 30 min) prevents LPA-induced endocytosis of Kv1.2. Y27632 when applied alone significantly increases surface Kv1.2 levels above that of saline control (n = 40; *p < 0.01, **p < 0.001). LPA had no significant effect in cells pretreated with Y27632. Left, inset, two-way ANOVA indicates that the percentage of change in surface channel elicited by LPA in control cells was significantly different from that elicited in the presence of Y27632 (n = 30; **p < 0.01). Inset, right, application of LPA (10 μM; 15 min) stimulates ROCK activity, whereas application of Y27632 inhibits ROCK activity as measured by immunoblot of phosphorylated MYPT1. Phospho-MYPT1 was detected with α-pMYPT1p. GAPDH was detected with α-GAPDHm as a loading control. Bar graph depicts quantification α-pMYPT1p normalized to GAPDH from three independent experiments. (C) In HEK-K cells, pretreatment with Y27632 blocks the translocation of Kv1.2 from the edge of cells to intracellular puncta upon stimulation with LPA. Surface Kv1.2 was labeled with α-Kv1.2e before stimulation with control saline or LPA.

Kv1.2 trafficking. LPA elicited a translocation of Kv1.2 from the cell periphery to intracellular puncta, indicative of channel endocytosis (Nesti *et al.*, 2004), an effect completely blocked by Y27632. Collectively, these findings indicate that ROCK is an essential downstream effector for receptor-induced, RhoA-mediated endocytosis of Kv1.2. Because both ROCK (RB/PH-TT) overexpression and Y27632 treatment cause an increase of steady-state surface Kv1.2, these findings also indicate that basal ROCK activity is important downstream of RhoA for maintaining steady-state Kv1.2 at the cell surface as well.

LPA-induced Kv1.2 Endocytosis Is Clathrin Dependent
Although Kv1.2 endocytosis can be elicited by a variety of stimuli (Huang *et al.*, 1993; Nesti *et al.*, 2004; Williams *et al.*,

2007; Connors *et al.*, 2008), the specific endocytosis pathways involved are not known. Many cell surface proteins and ion channels are internalized in a clathrin-dependent manner, among them the Tf receptor, EGF receptor, as well as the epithelial sodium channel (Sorkin and Waters, 1993; Shimkets *et al.*, 1997; Rotin *et al.*, 2001). We therefore sought to explore the role of clathrin in the RhoA/ROCK-mediated endocytosis of Kv1.2. Knockdown of clathrin protein with siRNA inhibits Tf receptor internalization (Hinrichsen *et al.*, 2003). We therefore chose this approach to explore the role of clathrin in Kv1.2 endocytosis. To validate the efficacy of clathrin siRNA in HEK-K cells, clathrin protein levels were determined in cells transfected with nontargeting (NT) siRNA or with siRNA targeting clathrin. Transfection of clathrin siRNA reduced clathrin protein levels by 50% com-

Figure 4. LPA-induced endocytosis of Kv1.2 is clathrin dependent. (A) Transfection of HEK-K cells with siRNA directed against the heavy chain of human clathrin depletes clathrin protein by 50% compared with nontargeting siRNA control. Clathrin heavy chain protein was detected with α-CHCm. GAPDH was detected with α-GAPDHm as a loading control. Bar graph represents quantification of eight individual experiments (n = 8; *p = 0.008). (B) Immunofluorescence of single optical slices through the center of HEK-K cells illustrates that clathrin siRNA reduces clathrin signal intensity and reduced the number of internalized Alexa Fluor 488-conjugated transferrin-containing puncta compared with nontargeting control both at 0- and 15-min incubation at 37°C. Clathrin heavy chain was detected with α-CHCm. (C) Quantitation of immunofluorescence images reveals that clathrin siRNA reduces clathrin signal intensity by ~30% compared with nontargeting control (n = 37; *p = 0.035). (D) Quantitation of immunofluorescence images reveals that transferrin uptake is reduced threefold in cells with clathrin siRNA compared with cells with nontargeting siRNA control (n = 17; *p < 0.05, **p < 0.001). (E) Flow cytometric analysis of HEK-K cells reveals that clathrin siRNA reduces LPA-induced endocytosis of Kv1.2, while having no effect on steady-state surface Kv1.2 levels. Treatment with Y27632 (10 μM; 30 min) significantly increases surface Kv1.2 both in the absence or presence of clathrin siRNA (n = 33; *p < 0.05, **p < 0.001). Inset, left, LPA-induced Kv1.2 endocytosis is significantly reduced in the presence of clathrin siRNA (n = 33; *p < 0.05). Inset, right, effect of Y27632 is not significantly altered in the absence or presence of clathrin siRNA (n = 33; p = 0.493). (F) Inhibiting clathrin dependent endocytosis with chlorpromazine or hypertonic sucrose inhibits LPA-induced KV1.2 endocytosis. The percentage of reduction in surface Kv1.2 elicited by LPA in control cells was significant (n = 26; *p < 0.01); however, LPA had no significant effect in cells pretreated with chlorpromazine (n = 18; p = 0.21) or by hypertonic sucrose (n = 9; p = 0.19).

pared with cells transfected with NT RNAi, as detected by immunoblot (Figure 4A) (n = 8; **p = 0.008). Comparable results were obtained from immunofluorescence experiments (Figure 4C), in which clathrin signal intensity was reduced by 30% compared with NT control (Figure 4C) (n = 37; *p = 0.035). Although incomplete, this level of reduction was sufficient to interfere with clathrin-dependent endocytosis because Tf receptor internalization, as viewed by immunofluorescence (Figure 4B), was reduced approximately threefold in cells transfected with clathrin siRNA compared with NT siRNA control (Figure 4D) (n = 17; *p < 0.05, **p < 0.001). Thus, knockdown of clathrin protein in HEK-K cells is an effective way to inhibit clathrin-dependent endocytosis. Continuing with this technique, we found that knockdown of clathrin heavy chain produced a significant inhibition of LPA induced Kv1.2 endocytosis relative to cells transfected with a nontargeting RNAi (*p < 0.001) (Figure 4E, left inset). This incomplete but significant inhibition is similar in degree to the incomplete but significant knockdown of clathrin protein by siRNA transfection. To confirm a role for clathrin in LPA-induced channel trafficking, we used two additional methods for inhibiting clathirin-dependent endocytosis: pretreatment with chlorpromazine (Wang *et al.*, 1993) or hypertonic sucrose (Heuser and Anderson, 1989). In control cells, LPA reduced surface channel by 28% (n = 26; *p < 0.001). However, LPA had no significant effect on surface channel levels in cells pretreatment with either chlorpromazine (30 μM; 30 min) (n = 18; p = 0.21) or hypertonic sucrose (0.5 M; 30 min) (n = 9; p = 0.19). Thus, three manipulations that interfere with clathrin-dependent endocytosis also significantly inhibit or eliminate LPA-induced Kv1.2 internalization. We conclude that LPA modulates Kv1.2 trafficking to a significant degree through a clathrin-dependent pathway. Interestingly, despite its effect on LPA-induced Kv1.2 endocytosis, clathrin knockdown had no detectable effect on the steady-state level of surface Kv1.2 and no effect on the ability of Y27632 to elevate surface Kv1.2 levels (Figure 4E, inset) (n = 33; p = 0.493). This suggests the intriguing hypothesis that LPA-induced endocytosis of Kv1.2 is clathrin dependent, whereas the trafficking mechanism responsible for maintaining the steady-state level of surface channel is clathrin-independent, despite both processes being regulated by RhoA/ROCK signaling.

Steady-State Endocytosis of Kv1.2 Is Cholesterol Dependent

We next sought to determine the trafficking pathway involved in the steady-state regulation of Kv1.2 at the cell surface. To assess the role of cholesterol in steady-state trafficking, we used the sterol-binding agent filipin to disrupt cholesterol-rich regions of the plasma membrane (Chang *et al.*, 1992; Rothberg *et al.*, 1992; Schnitzer *et al.*, 1994; Smart *et al.*, 1994). Steady-state surface levels of Kv1.2 were significantly increased in the presence of filipin, whereas subsequent Y27632 application had no additional effect (Figure 5A) (n = 32; *p < 0.01, **p < 0.001). In contrast, filipin did not block LPA-induced Kv1.2 endocytosis (Figure 5B) (n = 5; *p < 0.05, **p < 0.001). These findings also suggest that basal ROCK activity modulates steady-state surface Kv1.2. Additionally, cholesterol-dependent endocytosis operates constitutively, controlling the steady-state surface level of Kv1.2 independently of the clathrin-dependent endocytosis elicited by G protein-coupled LPA receptor stimulation.

In many instances, steady-state levels of proteins at the plasma membrane represent a homeostasis between endocytosis and recycling back to the plasma membrane (Dunn

and Hubbard, 1984; Morrison *et al.*, 1996; Leterrier *et al.*, 2004). Although filipin is widely used to block cholesterol-dependent endocytosis, it can have other effects on trafficking, including modulation of intracellular vesicular trafficking and recycling pathways (Kwik *et al.*, 2003). We therefore asked whether the effect of filipin on Kv1.2 involved one or both of these processes. To do so, we used low temperature (16°C) to inhibit vesicle trafficking and recycling. This manipulation leaves endocytosis from the plasma membrane intact (De Camilli *et al.*, 1995; Le and Nabi, 2003), thus enabling us to study channel recycling and channel endocytosis in relative isolation of one another. Incubation of HEK-K cells at 16°C for 1 h reduced steady-state surface Kv1.2 by ~50% relative to control cells maintained at 37°C (Figure 5E) (n = 27; **p < 0.001). This profound drop in surface Kv1.2 levels indicates that recycling does have a key role in the maintenance of surface Kv1.2 levels. In striking contrast, temperature inhibition of recycling did not impair the ability of filipin to potently increase the level of surface Kv1.2 (Figure 5C, inset) (n = 12; *p = 0.019, **p < 0.001). This finding confirms that basal surface Kv1.2 levels represent a homeostatic balance between two processes, cholesterol-dependent channel endocytosis and channel recycling back to the plasma membrane. However, it also raises the question of which branch of this homeostatic pathway is acted upon by ROCK. To address this, we used temperature inhibition of recycling in combination with ROCK inhibition. Temperature block eliminated the Y27632-induced increase of surface Kv1.2 (Figure 5D, inset) n ≥10; *p < 0.01, **p < 0.001), suggests that Y27623 and filipin increase surface Kv1.2 surface levels by distinct mechanisms; filipin by blocking channel endocytosis and Y27623 by increasing channel recycling back to the plasma membrane. Thus, this data suggests that RhoA/ROCK activity in unstimulated cells has a negative effect on surface Kv1.2 levels by inhibiting recycling of constitutively endocytosed channel back to the plasma membrane.

Dynamin Is Essential for Both Steady-State and LPA-induced Modulation of Kv1.2 Surface Levels

Dynamin is a small GTPase with a well-established role in both cholesterol-dependent and clathrin-dependent endocytosis (De Camilli *et al.*, 1995; Sever *et al.*, 2000). Our lab reported previously that tyrosine kinase-induced endocytosis of Kv1.2 is dynamin dependent (Nesti *et al.*, 2004). We therefore asked whether dynamin is also necessary for RhoA/ROCK-mediated endocytosis of Kv1.2. The small-molecule inhibitor dynasore (Macia *et al.*, 2006) was used to block the GTPase activity of dynamin. Increasing concentrations of dynasore applied to unstimulated HEK-K cells (30 min at 37°C) elicited a significant, concentration-dependent increase of surface Kv1.2 (Figure 6A) (n = 3; *p < 0.01, **p < 0.001). To ascertain the role of dynamin in stimulus-induced Kv1.2 trafficking, surface Kv1.2 levels were measured in LPA and Y27632-treated cells in the presence or absence of a maximal concentration of dynasore. Application of Y27632 (10 μM; 30 min) in control cells elicited a significant increase in surface channel levels; however, it had no effect in cells pretreated with 80 μM dynasore (Figure 6B) (n = 6; *p < 0.05, **p < 0.001). Similarly, LPA (10 μM; 15 min) caused a significant decrease in surface Kv1.2 levels in control cells, but its effect was abolished in cells pre-treated with dynasore (Figure 6B) (n = 6; *p < 0.05, **p < 0.001). We conclude that dynamin is necessary for both steady-state homeostasis of surface Kv1.2, and clathrin-dependent, LPA-induced Kv1.2 endocytosis.
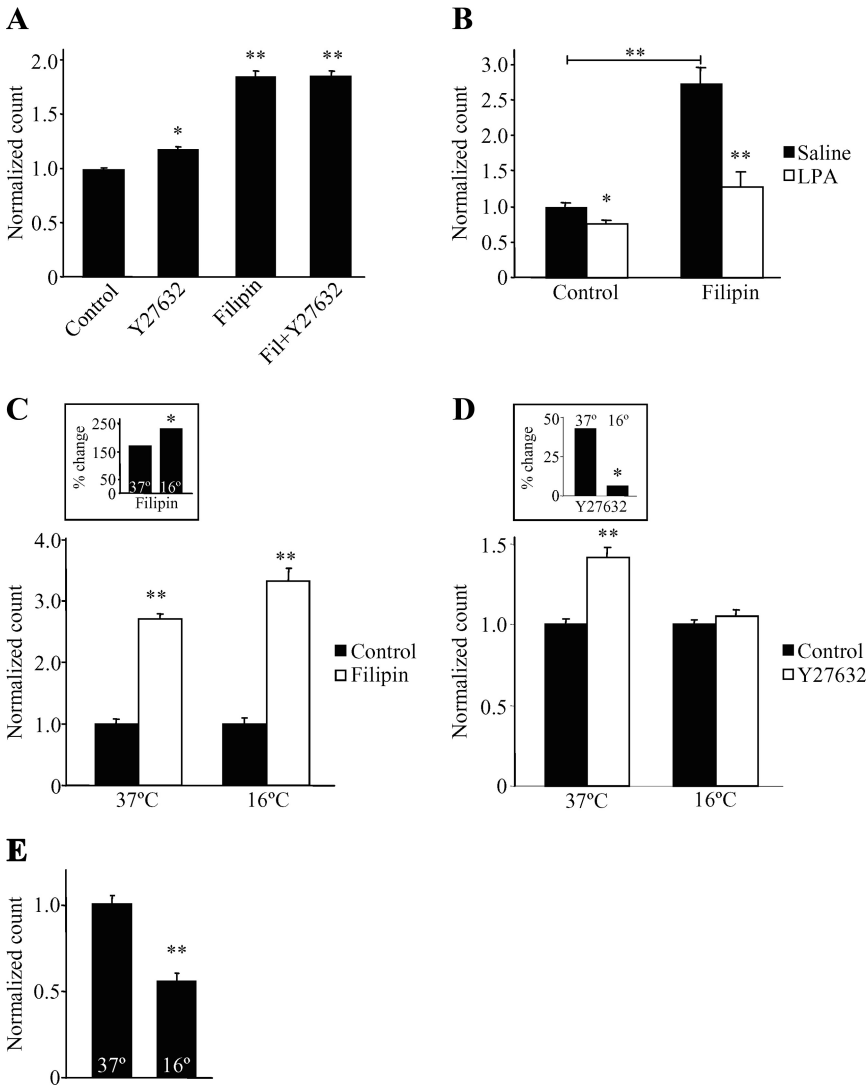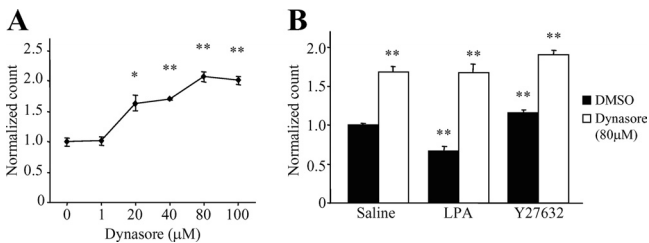
Figure 5. Steady-state Kv1.2 homeostasis is composed of constitutive cholesterol-dependent endocytosis and of constitutive recycling. (A) Application of the sterol-binding agent filipin (7.7 μM; 1 h) to HEK-K cells significantly increases steady-state surface Kv1.2 as detected by flow cytometry. Subsequent treatment with Y27632 (10 μM; 30 min) does not elicit a further increase (n = 32; *p < 0.01, **p < 0.001). (B) Filipin application does not prevent Kv1.2 endocytosis upon application of LPA (10 μM; 15 min) (n = 5; *p < 0.05, **p < 0.001). (C) Application of filipin (7.7 μM; 1 h) to HEK-K cells significantly increases surface Kv1.2 at both 37 and 16°C (n = 12; **p < 0.001). Inset, application of filipin at 16°C results in a significantly greater increase of surface Kv1.2 compared with 37°C control (n = 12; *p = 0.019). (D) Y27632 (10 μM; 30 min) does not elicit an increase of steady-state surface Kv1.2 at 16°C (n ≥10; **p < 0.001). Inset, percentage of increase in surface Kv1.2 elicited by Y27632 at 37 versus 16°C is significantly different (n ≥10, *p < 0.01). (E) Incubation at 16°C results in significantly reduced levels of steady-state surface Kv1.2 compared with 37°C control (n = 27; **p < 0.001).

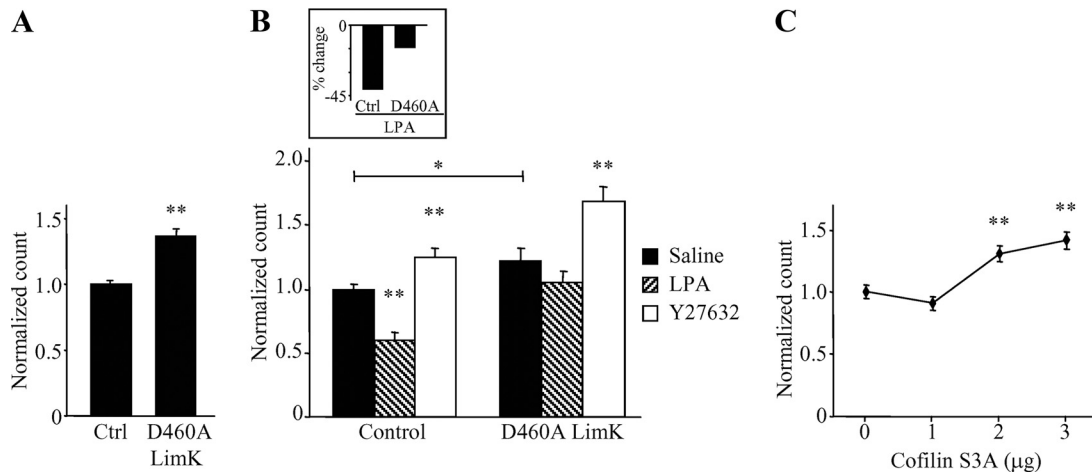### LIM-Kinase/Cofilin Is Implicated in ROCK-dependent Modulation of Kv1.2

Previous studies have indicated a role for actin remodeling by the Arp 2/3 protein complex in Kv1.2 trafficking (Hattan *et al.*, 2002; Williams *et al.*, 2007; Connors *et al.*, 2008). This was intriguing because cofilin, an actin-severing protein, also interacts with Arp 2/3 to remodel actin (Ichetovkin *et al.*, 2002). The actin-severing activity of cofilin is regulated through phosphorylation-dependent inhibition by LIM-kinase (LIMK), which itself can be activated by ROCK (Bernard, 2007). We therefore assessed the role of LIMK in Kv1.2 trafficking by overexpressing a dominant-negative LIMK (D460A) that lacks kinase activity (Matsui *et al.*, 2002). In unstimulated HEK-K cells, steady-state levels of surface Kv1.2 are significantly increased in the presence of LIMK (D460A) (Figure 7A) (n = 78; **p < 0.001). When LPA was applied (10 μM; 15 min) in the presence of LIMK (D460A), loss of surface Kv1.2 was blocked (Figure 7B: n = 21; p̂ < 0.05, *p < 0.01, **p < 0.001; and Figure 7B, inset: n = 21; *p < 0.05). The Y27632-induced increase of surface Kv1.2 was not significantly affected by overexpression of LIMK (D460A) (Figure 7B, inset) (n = 21, p = 0.143). In addition, transfection of increasing amounts of DNA encoding an active form of cofilin (S3A) that cannot be phosphorylated and deactivated by LIMK (Arber *et al.*, 1998) results in a concentration-dependent increase of steady-state surface Kv1.2 (Figure 7C) (n = 12; *p < 0.01, **p < 0.001). Overexpression of active cofilin was designed to

Figure 6. Dynamin is essential for Kv1.2 trafficking. (A) Treatment of unstimulated HEK-K cells with increasing concentrations of dynasore (30 min at 37°C) results in a significant, concentration-dependent increase in steady-state surface Kv1.2 as detected by flow cytometry (n = 3; *p < 0.01, **p < 0.001). (B) LPA (10 μM; 15 min) and Y27632 (10 μM; 30 min) have no effect in the presence of 80 μM dynasore (n = 6; *p < 0.05, **p < 0.001).

A **B** **C**

Figure 7. LIM kinase and cofilin control surface expression of Kv1.2 downstream of ROCK. (A) Overexpression of a dominant-negative form of LIM kinase 1 (D460A) significantly increases steady-state surface Kv1.2 in HEK-K cells as detected by flow cytometry (n = 78; **$p < 0.001$). (B) LIM kinase 1 (D460A) reduces LPA-induced endocytosis of Kv1.2. Y27632 (10 μM; 30 min) elicits an increase in surface Kv1.2 in the absence or presence of LIM kinase 1 (D460A) (n = 21; ŷ < 0.05, *$p < 0.01$, **$p < 0.001$). Inset, in the presence of LIM kinase 1 (D460A), LPA-induced Kv1.2 endocytosis is significantly reduced (n = 21; *$p < 0.05$). (C) Transient transfection of HEK-K cells with increasing amounts of DNA encoding a constitutively active form of cofilin (S3A) significantly increases steady-state surface Kv1.2 in a concentration-dependent manner (n = 12, *$p < 0.01$, **$p < 0.001$).

mimic the presence of LIMK (D460A). These results suggest the LIMK/cofilin pathway contributes to RhoA-mediated Kv1.2 suppression via LPA receptor activation.

DISCUSSION

Potassium channel regulation is a fundamental means for controlling cellular excitability. In this study, we report that RhoA signals through ROCK to regulate potassium ion channel trafficking. We show that the Kv1.2 potassium channel is subject to two independent forms of trafficking at the plasma membrane, one modulates the homeostasis of Kv1.2 at the cell surface and the other results in acute Kv1.2 endocytosis after G protein-coupled receptor activation. Intriguingly, we find that RhoA/ROCK has a central role in both forms but that it affects distinct stages of trafficking for each. Stimulated endocytosis of Kv1.2 is clathrin-dependent and requires RhoA/ROCK. In contrast, RhoA/ROCK seems to modulate steady-state surface homeostasis, which involves cholesterol-dependent trafficking, not at the internalization stage, but by inhibiting Kv1.2 recycling back to the plasma membrane. This study therefore not only unites two previous studies, one showing that RhoA has a central role in the tyrosine kinase-dependent suppression of Kv1.2 ionic current (Huang et al., 1993) and the other identifying endocytosis as a key mechanism for the suppression of Kv1.2 (Nesti et al., 2004), it also provides new insight into the complex RhoA in regulating membrane protein trafficking in general.

Using both pharmacological inhibition and overexpression of dominant-negative RhoA, we have shown that RhoA activity inversely correlates to the level of Kv1.2 at the cell surface. Application of C3 exoenzyme or overexpression of a dominant-negative form of RhoA both caused significant and dose-dependent increases in Kv1.2 present at the cell surface (Figure 1, A and B). C3 exoenzyme also blocked steady-state internalization of Kv1.2 (Figure 1C), demonstrating that RhoA is required for steady state Kv1.2 endocytosis. Therefore, the increase in surface Kv1.2 caused by inhibition of RhoA likely resulted from continued accumulation of Kv1.2 on the cell surface from a recycling pathway

still active in the absence of steady-state endocytosis. In addition to regulating steady-state Kv1.2 trafficking, RhoA is essential for acute regulation of channel trafficking as well because inhibition of RhoA with C3 exoenzyme completely blocked LPA receptor induced Kv1.2 endocytosis (Figure 2). This is consistent with other studies showing that LPA receptors can couple to $G_{12/13}$ to activate RhoA (Moolenaar, 1995; Bian et al., 2006). It is also consistent with pervious work linking suppression of Kv1.2 ionic current to the activation of RhoA by M1 muscarinic acetylcholine receptors (Cachero et al., 1998). Thus, RhoA has a key role in both steady-state and receptor-induced Kv1.2 trafficking.

Although several studies have examined the relationship between Kv1.2 function and its endocytosis (Nesti et al., 2004; Williams et al., 2007; Connors et al., 2008), the mechanisms by which Kv1.2 undergoes endocytosis remained unclear. A previous report (Williams et al., 2007) as well as the data shown in Figures 1 and 2 indicate that expression of Kv1.2 in the plasma membrane is subject to steady-state and acute regulation. Here, we report that steady-state regulation of Kv1.2 involves cholesterol-dependent channel internalization and that acute, receptor-stimulated endocytosis proceeds through a separate, clathrin-dependent mechanism. These studies use a combination of clathrin knockdown and cholesterol sequestration to functionally isolate these two pathways. In Figure 5, we show that application of the sterol-binding agent filipin caused an accumulation of Kv1.2 at the cell surface. It is notable that filipin does not block LPA-induced channel endocytosis despite having blocked cholesterol-mediated endocytosis (Figure 5B, inset). This result could be explained if more than one pool of Kv1.2 exists. A pool of Kv1.2 subject to cholesterol-dependent endocytosis may be isolated from the clathrin endocytosis machinery, possibly by being sequestered in lipid rafts. Disruption of those rafts with filipin would have then made additional channel available for endocytosis by the clathrin-dependent pathway activated by LPA receptor stimulation. Localization of Kv1.2 to cholesterol-rich domains is plausible given that such localization has been demonstrated for the closely related channels Kv1.3 and Kv1.5 (Martens et al.,

2001; Martinez-Marmol *et al.*, 2008; Vicente *et al.*, 2008). We also note that clathrin-dependent endocytosis can also be affected by depletion of cholesterol. In Figure 4 we show that inhibition of clathrin dependent endocytosis did not alter the level of steady-state surface Kv1.2 but did inhibit LPA-induced channel endocytosis. Therefore, in this experimental system, filipin and clathrin siRNA are effective means of functionally isolating cholesterol and clathrin-dependent endocytosis.

The contribution of RhoA/ROCK to clathrin-dependent endocytosis is well established (Muro *et al.*, 2003; Nishimura *et al.*, 2003; Samaniego *et al.*, 2007). The role of RhoA/ROCK in cholesterol-dependent endocytosis is less well studied but also has been described previously (Mayor and Pagano, 2007). We show that although RhoA/ROCK affects both pathways in the regulation of Kv1.2, the mechanisms by which it does so are distinct. Using low temperature to inhibit steady-state homeostatic vesicle recycling, we found that compared with 37°C, surface Kv1.2 levels are significantly reduced at 16°C but remained sensitive to cholesterol sequestration with filipin (Figure 5C), indicating that filipin blocks steady-state endocytosis but not recycling. Remarkably, although it had no apparent effect on the ability of filipin to increase surface Kv1.2 levels, low temperature significantly inhibited the ability of Y2763 to increase surface Kv1.2 levels. This suggests that basal ROCK activity functions as a negative regulator of Kv1.2 recycling to the plasma membrane. We also note that our results indicate that recycling of Kv1.2 is reduced but not eliminated at low temperature. The combination of ongoing endocytosis and inhibited recycling would be expected to cause a net decrease in surface levels of Kv1.2, as show in Figure 5E. However, inhibiting steady-state endocytosis with filipin could increase surface channel levels even at low temperature, as shown in Figure 5C, because even sharply reduced recycling could still cause accumulation on the cell surface when endocytosis is blocked. This finding is consistent with other studies showing impaired but not complete block of recycling at low temperatures (Punnonen *et al.*, 1998; van Dam *et al.*, 2005). Collectively, these findings indicate that steady-state Kv1.2 levels are governed by a homeostatic balance between cholesterol-dependent channel endocytosis and subsequent recycling back to the plasma membrane and that steady-state RhoA/ROCK signaling affects primarily the recycling component of this pathway.

Clathrin-dependent endocytosis is, generally, dynamin-dependent. In contrast, clathrin-independent modes of endocytosis can proceed with or without a requirement for dynamin (Mayor and Pagano, 2007). In a previous study, Kv1.2 endocytosis via muscarinic acetylcholine receptor stimulation was reported to be dynamin-dependent (Nesti *et al.*, 2004). Here, we show that inhibition of the GTPase activity of dynamin with the small-molecule inhibitor dynasore (Macia *et al.*, 2006) blocks both constitutive and LPA-induced Kv1.2 endocytosis (Figure 6). Because receptor-induced and steady-state Kv1.2 trafficking occur through distinct mechanisms, it is likely that dynamin has different functional roles in each case. We believe that the most likely mechanism for dynamin in LPA-induced channel endocytosis is through its classical role as a pinchase for clathrin-coated vesicles (Danino *et al.*, 2004). The roles of dynamin in other forms of trafficking are less clear, although mounting evidence indicates that it has a key role in intracellular vesicle trafficking by modulating actin dynamics in coordination with cortactin (McNiven *et al.*, 2000; Krueger *et al.*, 2003; Cao *et al.*, 2005). We note that a previous study identified distinct domains within cortactin that are required for

the independent regulation of steady-state or receptor induced Kv1.2 trafficking (Williams *et al.*, 2007). Collectively, these findings raise the intriguing possibility that RhoA, cortactin, and dynamin act in concert to regulate channel trafficking through their effects on actin dynamics.

The idea that RhoA/ROCK affects channel trafficking through an actin-dependent mechanism is shown more directly with our finding that ROCK modulates Kv1.2 trafficking through LIM-kinase/cofilin (Figure 7). Expression of a dominant-negative form of LIM-kinase or an active form of cofilin elicits an increase in steady-state surface channel levels. Dominant-negative LIM-kinase also significantly reduces the LPA-induced suppression of Kv1.2. Strikingly, dominant-negative LIM-kinase had no significant effect on the elevation of surface Kv1.2 levels that occurs after ROCK inhibition with Y27632. We speculate that LIM-kinase affects the internalization phase of the steady-state and receptor-induced pathways for Kv1.2 endocytosis, but not ROCK-dependent Kv1.2 recycling, although confirmation of this idea awaits further study. This hypothesis is consistent with other reports of a requirement for LIM-kinase activity in the internalization of β-adrenergic (Volovyk *et al.*, 2006) and the EGF (Nishimura *et al.*, 2004) receptors, as well as reports that LIM kinase can be activated by multiple upstream proteins in addition to ROCK (Edwards *et al.*, 1999; Dan *et al.*, 2001; Sumi *et al.*, 2001). We also note that involvement of LIM-kinase/cofilin in both the steady-state and receptor-induced trafficking of Kv1.2 is particularly informative in view of a similar dual role for the actin regulating protein cortactin (Williams *et al.*, 2007). This convergence at the level of Kv1.2 trafficking, as well as the reported ability of cofilin and cortactin to act in concert to regulate actin dynamics (Yamaguchi and Condeelis, 2007; Lai *et al.*, 2008), suggests that Kv1.2 trafficking through both cholesterol and clathrin-dependent pathways involves a complex interaction of multiple actin-regulatory systems.

The concept that RhoA/ROCK can affect Kv1.2 trafficking in different ways in the same cell is consistent with previously described mechanisms for the regulation of Kv1.2. We have shown previously that cAMP can affect Kv1.2 trafficking in distinct ways depending on the degree of adenylate cyclase activation (Connors *et al.*, 2008). In another study we demonstrated that different functional domains within the actin binding protein cortactin have distinct effects on steady-state versus receptor induced Kv1.2 endocytosis (Williams *et al.*, 2007). In both cases, a single signaling entity was shown to modulate distinct aspects of Kv1.2 trafficking depending on the signaling environment within the cell. The data presented here suggest a similar multiplicity of roles for RhoA/ROCK in Kv1.2 regulation.

The discovery that RhoA/ROCK affects both the constitutive and stimulus-induced regulation of the same protein, Kv1.2, is significant because it broadens the overall view of how RhoA can regulate membrane protein trafficking. The finding that RhoA/ROCK can affect two modes of Kv1.2 trafficking also suggests a mechanism by which RhoA can differentially regulate membrane potential in response to distinct regulatory signals. In one instance, low levels of RhoA/ROCK activity could couple to a cholesterol-dependent Kv1.2 trafficking system, thereby affecting steady-state resting membrane potential. High levels of RhoA/ROCK, in contrast, could affect a parallel but distinct mechanism for Kv1.2 endocytosis requiring clathrin. We propose a model in which Kv1.2 surface expression, and thus activity, is modulated by the combined effects of multiple actin-regulating proteins, including dynamin, RhoA, and ROCK acting through distinct trafficking pathways.

REFERENCES

Adda, S., Fleischmann, B. K., Freedman, B. D., Yu, M., Hay, D. W., and Kotlikoff, M. I. (1996). Expression and function of voltage-dependent potassium channel genes in human airway smooth muscle. J. Biol. Chem. 271, 13239–13243.

Amano, M., Chihara, K., Nakamura, N., Kaneko, T., Matsuura, Y., and Kaibuchi, K. (1999). The COOH terminus of Rho-kinase negatively regulates rho-kinase activity. J. Biol. Chem. 274, 32418–32424.

Arber, S., Barbayannis, F. A., Hanser, H., Schneider, C., Stanyon, C. A., Bernard, O., and Caroni, P. (1998). Regulation of actin dynamics through phosphorylation of cofilin by LIM-kinase. Nature 393, 805–809.

Bernard, O. (2007). Lim kinases, regulators of actin dynamics. Int. J. Biochem. Cell Biol. 39, 1071–1076.

Bian, D., Mahanivong, C., Yu, J., Frisch, S. M., Pan, Z. K., Ye, R. D., and Huang, S. (2006). The G12/13-RhoA signaling pathway contributes to efficient lysophosphatidic acid-stimulated cell migration. Oncogene 25, 2234–2244.

Brew, H. M., et al. (2007). Seizures and reduced life span in mice lacking the potassium channel subunit Kv1.2, but hypoexcitability and enlarged Kv1 currents in auditory neurons. J Neurophysiol 98, 1501–1525.

Cachero, T. G., Morielli, A. D., and Peralta, E. G. (1998). The small GTP-binding protein RhoA regulates a delayed rectifier potassium channel. Cell 93, 1077–1085.

Cao, H., Weller, S., Orth, J. D., Chen, J., Huang, B., Chen, J. L., Stamnes, M., and McNiven, M. A. (2005). Actin and Arf1-dependent recruitment of a cortactin-dynamin complex to the Golgi regulates post-Golgi transport. Nat. Cell Biol. 7, 483–492.

Chang, W. J., Rothberg, K. G., Kamen, B. A., and Anderson, R. G. (1992). Lowering the cholesterol content of MA104 cells inhibits receptor-mediated transport of folate. J. Cell Biol. 118, 63–69.

Connors, E. C., Ballif, B. A., and Morielli, A. D. (2008). Homeostatic regulation of Kv1.2 potassium channel trafficking by cyclic AMP. J. Biol. Chem. 283, 3445–3453.

Cox, R. H., Folander, K., and Swanson, R. (2001). Differential expression of voltage-gated K(+) channel genes in arteries from spontaneously hypertensive and Wistar-Kyoto rats. Hypertension 37, 1315–1322.

Dada, L. A., Novoa, E., Lecuona, E., Sun, H., and Sznajder, J. I. (2007). Role of the small GTPase RhoA in the hypoxia-induced decrease of plasma membrane Na,K-ATPase in A549 cells. J. Cell Sci. 120, 2214–2222.

Dan, C., Kelly, A., Bernard, O., and Minden, A. (2001). Cytoskeletal changes regulated by the PAK4 serine/threonine kinase are mediated by LIM kinase 1 and cofilin. J. Biol. Chem. 276, 32115–32121.

Danino, D., Moon, K. H., and Hinshaw, J. E. (2004). Rapid constriction of lipid bilayers by the mechanochemical enzyme dynamin. J. Struct. Biol. 147, 259–267.

De Camilli, P., Takei, K., and McPherson, P. S. (1995). The function of dynamin in endocytosis. Curr. Opin. Neurobiol. 5, 559–565.

Dodson, P. D., Billups, B., Rusznak, Z., Szucs, G., Barker, M. C., and Forsythe, I. D. (2003). Presynaptic rat Kv1.2 channels suppress synaptic terminal hyperexcitability following action potential invasion. J. Physiol. 550, 27–33.

Dunn, W. A., and Hubbard, A. L. (1984). Receptor-mediated endocytosis of epidermal growth factor by hepatocytes in the perfused rat liver: ligand and receptor dynamics. J. Cell Biol. 98, 2148–2159.

Edwards, D. C., Sanders, L. C., Bokoch, G. M., and Gill, G. N. (1999). Activation of LIM-kinase by Pak1 couples Rac/Cdc42 GTPase signalling to actin cytoskeletal dynamics. Nat. Cell Biol. 1, 253–259.

Feng, J., Ito, M., Ichikawa, K., Isaka, N., Nishikawa, M., Hartshorne, D. J., and Nakano, T. (1999). Inhibitory phosphorylation site for Rho-associated kinase on smooth muscle myosin phosphatase. J. Biol. Chem. 274, 37385–37390.

Grosse, G., Draguhn, A., Hohne, L., Tapp, R., Veh, R. W., and Ahnert-Hilger, G. (2000). Expression of Kv1 potassium channels in mouse hippocampal primary cultures: development and activity-dependent regulation. J. Neurosci. 20, 1869–1882.

Haghdoust, H., Janahmadi, M., and Behzadi, G. (2007). Physiological role of dendrotoxin-sensitive K+ channels in the rat cerebellar Purkinje neurons. Physiol. Res. 56, 807–813.

Hattan, D., Nesti, E., Cachero, T. G., and Morielli, A. D. (2002). Tyrosine phosphorylation of Kv1.2 modulates its interaction with the actin-binding protein cortactin. J. Biol. Chem. 277, 38596–38606.

Heuser, J. E., and Anderson, R. G. (1989). Hypertonic media inhibit receptor-mediated endocytosis by blocking clathrin-coated pit formation. J. Cell Biol. 108, 389–400.

Hinrichsen, L., Harborth, J., Andrees, L., Weber, K., and Ungewickell, E. J. (2003). Effect of clathrin heavy chain- and alpha-adaptin-specific small inhibitory RNAs on endocytic accessory proteins and receptor trafficking in HeLa cells. J. Biol. Chem. 278, 45160–45170.

Hong, Z., Weir, E. K., Nelson, D. P., and Olschewski, A. (2004). Subacute hypoxia decreases voltage-activated potassium channel expression and function in pulmonary artery myocytes. Am. J. Respir. Cell Mol. Biol. 31, 337–343.

Huang, X. Y., Morielli, A. D., and Peralta, E. G. (1993). Tyrosine kinase-dependent suppression of a potassium channel by the G protein-coupled m1 muscarinic acetylcholine receptor. Cell 75, 1145–1156.

Ichetovkin, I., Grant, W., and Condeelis, J. (2002). Cofilin produces newly polymerized actin filaments that are preferred for dendritic nucleation by the Arp2/3 complex. Curr. Biol. 12, 79–84.

Ishikawa, K., Tanaka, M., Black, J. A., and Waxman, S. G. (1999). Changes in expression of voltage-gated potassium channels in dorsal root ganglion neurons following axotomy. Muscle Nerve 22, 502–507.

Ishizaki, T., et al. (1996). The small GTP-binding protein Rho binds to and activates a 160 kDa Ser/Thr protein kinase homologous to myotonic dystrophy kinase. EMBO J. 15, 1885–1893.

Kaneko, T., Maeda, A., Takefuji, M., Aoyama, H., Nakayama, M., Kawabata, S., Kawano, Y., Iwamatsu, A., Amano, M., and Kaibuchi, K. (2005). Rho mediates endocytosis of epidermal growth factor receptor through phosphorylation of endophilin A1 by Rho-kinase. Genes Cells 10, 973–987.

Kim, D. S., Choi, J. O., Rim, H. D., and Cho, H. J. (2002). Downregulation of voltage-gated potassium channel alpha gene expression in dorsal root ganglia following chronic constriction injury of the rat sciatic nerve. Brain Res. Mol. Brain Res. 105, 146–152.

Krueger, E. W., Orth, J. D., Cao, H., and McNiven, M. A. (2003). A dynamin-cortactin-Arp2/3 complex mediates actin reorganization in growth factor-stimulated cells. Mol. Biol. Cell 14, 1085–1096.

Kwik, J., Boyle, S., Fooksman, D., Margolis, L., Sheetz, M. P., and Edidin, M. (2003). Membrane cholesterol, lateral mobility, and the phosphatidylinositol 4,5-bisphosphate-dependent organization of cell actin. Proc. Natl. Acad. Sci. USA 100, 13964–13969.

Lai, F. P., Szczodrak, M., Block, J., Faix, J., Breitsprecher, D., Mannherz, H. G., Stradal, T. E., Dunn, G. A., Small, J. V., and Rottner, K. (2008). Arp2/3 complex interactions and actin network turnover in lamellipodia. EMBO J. 27, 982–992.

Lamaze, C., Chuang, T. H., Terlecky, L. J., Bokoch, G. M., and Schmid, S. L. (1996). Regulation of receptor-mediated endocytosis by Rho and Rac. Nature 382, 177–179.

Lambe, E. K., and Aghajanian, G. K. (2001). The role of Kv1.2-containing potassium channels in serotonin-induced glutamate release from thalamocortical terminals in rat frontal cortex. J. Neurosci. 21, 9955–9963.

Laube, G., Roper, J., Pitt, J. C., Sewing, S., Kistner, U., Garner, C. C., Pongs, O., and Veh, R. W. (1996). Ultrastructural localization of Shaker-related potassium channel subunits and synapse-associated protein 90 to septate-like junctions in rat cerebellar Pinceaux. Brain Res. Mol. Brain Res 42, 51–61.

Le, P. U., and Nabi, I. R. (2003). Distinct caveolae-mediated endocytic pathways target the Golgi apparatus and the endoplasmic reticulum. J. Cell Sci. 116, 1059–1071.

Leterrier, C., Bonnard, D., Carrel, D., Rossier, J., and Lenkei, Z. (2004). Constitutive endocytic cycle of the CB1 cannabinoid receptor. J. Biol. Chem. 279, 36013–36021.

Luykenaar, K. D., Brett, S. E., Wu, B. N., Wiehler, W. B., and Welsh, D. G. (2004). Pyrimidine nucleotides suppress KDR currents and depolarize rat cerebral arteries by activating Rho kinase. Am. J. Physiol. Heart Circ. Physiol. 286, H1088–H1100.

Macia, E., Ehrlich, M., Massol, R., Boucrot, E., Brunner, C., and Kirchhausen, T. (2006). Dynasore, a cell-permeable inhibitor of dynamin. Dev. Cell *10*, 839–850.

Martens, J. R., Sakamoto, N., Sullivan, S. A., Grobaski, T. D., and Tamkun, M. M. (2001). Isoform-specific localization of voltage-gated K+ channels to distinct lipid raft populations. Targeting of Kv1.5 to caveolae. J. Biol. Chem. *276*, 8409–8414.

Martinez-Marmol, R., Villalonga, N., Sole, L., Vicente, R., Tamkun, M. M., Soler, C., and Felipe, A. (2008). Multiple Kv1.5 targeting to membrane surface microdomains. J. Cell. Physiol. *217*, 667–673.

Matsui, S., Matsumoto, S., Adachi, R., Kusui, K., Hirayama, A., Watanabe, H., Ohashi, K., Mizuno, K., Yamaguchi, T., Kasahara, T., and Suzuki, K. (2002). LIM kinase 1 modulates opsonized zymosan-triggered activation of macrophage-like U937 cells. Possible involvement of phosphorylation of cofilin and reorganization of actin cytoskeleton. J. Biol. Chem. *277*, 544–549.

Matsui, T., Amano, M., Yamamoto, T., Chihara, K., Nakafuku, M., Ito, M., Nakano, T., Okawa, K., Iwamatsu, A., and Kaibuchi, K. (1996). Rho-associated kinase, a novel serine/threonine kinase, as a putative target for small GTP binding protein Rho. EMBO J. *15*, 2208–2216.

Mayor, S., and Pagano, R. E. (2007). Pathways of clathrin-independent endocytosis. Nat. Rev. Mol. Cell Biol. *8*, 603–612.

McNiven, M. A., Kim, L., Krueger, E. W., Orth, J. D., Cao, H., and Wong, T. W. (2000). Regulated interactions between dynamin and the actin-binding protein cortactin modulate cell shape. J. Cell Biol. *151*, 187–198.

Moolenaar, W. H. (1995). Lysophosphatidic acid signalling. Curr. Opin. Cell Biol. *7*, 203–210.

Morrison, K. J., Moore, R. H., Carsrud, N. D., Trial, J., Millman, E. E., Tuvim, M., Clark, R. B., Barber, R., Dickey, B. F., and Knoll, B. J. (1996). Repetitive endocytosis and recycling of the beta 2-adrenergic receptor during agonist-induced steady state redistribution. Mol. Pharmacol. *50*, 692–699.

Muro, S., Wiewrodt, R., Thomas, A., Koniaris, L., Albelda, S. M., Muzykantov, V. R., and Koval, M. (2003). A novel endocytic pathway induced by clustering endothelial ICAM-1 or PECAM-1. J. Cell Sci. *116*, 1599–1609.

Nakamura, A., Hayashi, K., Ozawa, Y., Fujiwara, K., Okubo, K., Kanda, T., Wakino, S., and Saruta, T. (2003). Vessel- and vasoconstrictor-dependent role of rho/rho-kinase in renal microvascular tone. J. Vasc. Res. *40*, 244–251.

Narumiya, S., Ishizaki, T., and Watanabe, N. (1997). Rho effectors and reorganization of actin cytoskeleton. FEBS Lett. *410*, 68–72.

Nesti, E., Everill, B., and Morielli, A. D. (2004). Endocytosis as a mechanism for tyrosine kinase-dependent suppression of a voltage-gated potassium channel. Mol. Biol. Cell *15*, 4073–4088.

Nishimura, Y., Itoh, K., Yoshioka, K., Tokuda, K., and Himeno, M. (2003). Overexpression of ROCK in human breast cancer cells: evidence that ROCK activity mediates intracellular membrane traffic of lysosomes. Pathol. Oncol. Res. *9*, 83–95.

Nishimura, Y., Yoshioka, K., Bernard, O., Himeno, M., and Itoh, K. (2004). LIM kinase 1, evidence for a role in the regulation of intracellular vesicle trafficking of lysosomes and endosomes in human breast cancer cells. Eur. J. Cell Biol. *83*, 369–380.

Punnonen, E. L., Ryhanen, K., and Marjomaki, V. S. (1998). At reduced temperature, endocytic membrane traffic is blocked in multivesicular carrier endosomes in rat cardiac myocytes. Eur. J. Cell Biol. *75*, 344–352.

Rasband, M. N. (2004). It's "juxta" potassium channel! J. Neurosci. Res. *76*, 749–757.

Rasband, M. N., Park, E. W., Vanderah, T. W., Lai, J., Porreca, F., and Trimmer, J. S. (2001). Distinct potassium channels on pain-sensing neurons. Proc. Natl. Acad. Sci. USA *98*, 13373–13378.

Rasband, M. N., and Trimmer, J. S. (2001). Subunit composition and novel localization of K+ channels in spinal cord. J. Comp. Neurol. *429*, 166–176.

Rothberg, K. G., Heuser, J. E., Donzell, W. C., Ying, Y. S., Glenney, J. R., and Anderson, R. G. (1992). Caveolin, a protein component of caveolae membrane coats. Cell *68*, 673–682.

Rotin, D., Kanelis, V., and Schild, L. (2001). Trafficking and cell surface stability of ENaC. Am. J. Physiol. Renal Physiol. *281*, F391–F399.

Samaniego, R., Sanchez-Martin, L., Estecha, A., and Sanchez-Mateos, P. (2007). Rho/ROCK and myosin II control the polarized distribution of endocytic clathrin structures at the uropod of moving T lymphocytes. J. Cell Sci. *120*, 3534–3543.

Schnitzer, J. E., Oh, P., Pinney, E., and Allard, J. (1994). Filipin-sensitive caveolae-mediated transport in endothelium: reduced transcytosis, scavenger endocytosis, and capillary permeability of select macromolecules. J. Cell Biol. *127*, 1217–1232.

Sever, S., Damke, H., and Schmid, S. L. (2000). Dynamin:GTP controls the formation of constricted coated pits, the rate limiting step in clathrin-mediated endocytosis. J. Cell Biol. *150*, 1137–1148.

Sheng, M., Tsaur, M. L., Jan, Y. N., and Jan, L. Y. (1994). Contrasting subcellular localization of the Kv1.2 K+ channel subunit in different neurons of rat brain. J. Neurosci. *14*, 2408–2417.

Shimkets, R. A., Lifton, R. P., and Canessa, C. M. (1997). The activity of the epithelial sodium channel is regulated by clathrin-mediated endocytosis. J. Biol. Chem. *272*, 25537–25541.

Smart, E. J., Ying, Y. S., Conrad, P. A., and Anderson, R. G. (1994). Caveolin moves from caveolae to the Golgi apparatus in response to cholesterol oxidation. J. Cell Biol. *127*, 1185–1197.

Sorkin, A., and Waters, C. M. (1993). Endocytosis of growth factor receptors. Bioessays *15*, 375–382.

Southan, A. P., and Robertson, B. (1998). Patch-clamp recordings from cerebellar basket cell bodies and their presynaptic terminals reveal an asymmetric distribution of voltage-gated potassium channels. J. Neurosci. *18*, 948–955.

Subauste, M. C., Von Herrath, M., Benard, V., Chamberlain, C. E., Chuang, T. H., Chu, K., Bokoch, G. M., and Hahn, K. M. (2000). Rho family proteins modulate rapid apoptosis induced by cytotoxic T lymphocytes and Fas. J. Biol. Chem. *275*, 9725–9733.

Sumi, T., Matsumoto, K., Shibuya, A., and Nakamura, T. (2001). Activation of LIM kinases by myotonic dystrophy kinase-related Cdc42-binding kinase alpha. J. Biol. Chem. *276*, 23092–23096.

Symons, M., and Rusk, N. (2003). Control of vesicular trafficking by Rho GTPases. Curr. Biol. *13*, R409–R418.

Tsaur, M. L., Sheng, M., Lowenstein, D. H., Jan, Y. N., and Jan, L. Y. (1992). Differential expression of K+ channel mRNAs in the rat brain and down-regulation in the hippocampus following seizures. Neuron *8*, 1055–1067.

Uehata, M., *et al.* (1997). Calcium sensitization of smooth muscle mediated by a Rho-associated protein kinase in hypertension. Nature *389*, 990–994.

van Dam, E. M., Govers, R., and James, D. E. (2005). Akt activation is required at a late stage of insulin-induced GLUT4 translocation to the plasma membrane. Mol. Endocrinol. *19*, 1067–1077.

Veh, R. W., Lichtinghagen, R., Sewing, S., Wunder, F., Grumbach, I. M., and Pongs, O. (1995). Immunohistochemical localization of five members of the Kv1 channel subunits: contrasting subcellular locations and neuron-specific co-localizations in rat brain. Eur. J. Neurosci. *7*, 2189–2205.

Vicente, R., Villalonga, N., Calvo, M., Escalada, A., Solsona, C., Soler, C., Tamkun, M. M., and Felipe, A. (2008). Kv1.5 association modifies Kv1.3 traffic and membrane localization. J. Biol. Chem. *283*, 8756–8764.

Volovyk, Z. M., Wolf, M. J., Prasad, S. V., and Rockman, H. A. (2006). Agonist-stimulated beta-adrenergic receptor internalization requires dynamic cytoskeletal actin turnover. J. Biol. Chem. *281*, 9773–9780.

Wang, J., Juhaszova, M., Rubin, L. J., and Yuan, X. J. (1997). Hypoxia inhibits gene expression of voltage-gated K+ channel alpha subunits in pulmonary artery smooth muscle cells. J. Clin. Invest. *100*, 2347–2353.

Wang, J., Weigand, L., Wang, W., Sylvester, J. T., and Shimoda, L. A. (2005). Chronic hypoxia inhibits Kv channel gene expression in rat distal pulmonary artery. Am. J. Physiol. Lung Cell Mol. Physiol. *288*, L1049–L1058.

Wang, L. H., Rothberg, K. G., and Anderson, R. G. (1993). Mis-assembly of clathrin lattices on endosomes reveals a regulatory switch for coated pit formation. J. Cell Biol. *123*, 1107–1117.

Williams, M. R., Markey, J. C., Doczi, M. A., and Morielli, A. D. (2007). An essential role for cortactin in the modulation of the potassium channel Kv1.2. Proc. Natl. Acad. Sci. USA *104*, 17412–17417.

Yamaguchi, H., and Condeelis, J. (2007). Regulation of the actin cytoskeleton in cancer cell migration and invasion. Biochim. Biophys. Acta *1773*, 642–652.

Yang, E. K., Takimoto, K., Hayashi, Y., de Groat, W. C., and Yoshimura, N. (2004). Altered expression of potassium channel subunit mRNA and alpha-dendrotoxin sensitivity of potassium currents in rat dorsal root ganglion neurons after axotomy. Neuroscience *123*, 867–874.

Yuan, X. J. (1995). Voltage-gated K+ currents regulate resting membrane potential and [Ca2+]i in pulmonary arterial myocytes. Circ. Res. *77*, 370–378.

Yuan, X. J., Wang, J., Juhaszova, M., Golovina, V. A., and Rubin, L. J. (1998). Molecular basis and function of voltage-gated K+ channels in pulmonary arterial smooth muscle cells. Am. J Physiol. *274*, L621–L635.